3D Complex Padé FFD migration: A comparison of splitting techniques

Jessé C. Costa (UFPA & INCT-GP), Débora Mondini, Jörg Schleicher, Amélia Novais (UNICAMP & INCT-GP), Brazil

Copyright 2011, SBGf - Sociedade Brasileira de Geofísica.

This paper was prepared for presentation at the Twelfth International Congress of the Brazilian Geophysical Society, held in Rio de Janeiro, Brazil, August 15-18, 2011.

Contents of this paper were reviewed by the Technical Committee of the Twelfth International Congress of The Brazilian Geophysical Society and do not necessarily represent any position of the SBGf, its officers or members. Electronic reproduction or storage of any part of this paper for commercial purposes without the written consent of The Brazilian Geophysical Society is prohibited.

Abstract

Three-dimensional wave-equation migration techniques are quite expensive because of the huge matrices that need to be inverted. Many techniques have been proposed to reduce this cost by splitting the 3D problem into a sequence of 2D problems. We compare the performance of splitting techniques for stable 3D Fourier Finite-Difference (FFD) migration techniques in terms of image quality and computational cost. The FFD methods are complex Padé FFD and FFD plus interpolation, and the compared splitting techniques are two and four-way splitting as well as alternating four-way splitting, i.e., splitting into the coordinate directions at one depth and the diagonal directions at the next level. From numerical examples in homogeneous and inhomogeneous media, we conclude that alternate four-way splitting yields results of the same quality as full four-way splitting at the cost of two-way splitting.

Introduction

Because of its superiority in areas of complex geology, wave-equation migration is substituting Kirchhoff migration in practice. However, while Kirchhoff migration counts on more than 30 years of technological development, wave-equation migration methods still need to be improved in various aspects. One of these aspects is the efficient implementation of three-dimensional wave-equation migration.

The application of a three-dimensional wave-equation migration technique adds the problem of computational cost to those of stability and precision of the chosen migration algorithm. To speed up migration techniques like finite-difference (FD) (Claerbout, 1971) or Fourier finite-difference (FFD) migration (Ristow and Rühl, 1994), a technique known as splitting is frequently used. In this context, splitting means the separation of a single-step 3D migration into two 2D passes within planes parallel to the horizontal coordinate axes, usually the inline and crossline directions (Brown, 1983).

When splitting is applied to the implicit FD migration operator so that the equations are solved alternatingly in the inline and crossline directions, the resulting FD scheme is known as an Alternating-Direction-Implicit (ADI) scheme. This procedure has the drawback of being incorrect for strongly dipping reflectors, resulting in large positioning errors for this type of reflectors when the dip direction is away from the coordinate directions and thus outside the migration planes. This imprecision leads to numerical anisotropy, i.e., a migration operator that acts quite differently in different directions.

To improve this behaviour while retaining the advantages of a rather low computation cost, different procedures have been proposed. Ristow (1980, see also Ristow and Rühl, 1997) proposed to perform, in addition to the 2D migration in the coordinate planes, also 2D migrations in the diagonal directions between the coordinate axes. Kitchenside (1988) used phase-shift migration plus an additional FD propagation step of the residual field to reduce the splitting error. Graves and Clayton (1990) proposed the implementation of a phase-correction operator using FD and incorporating a damping function to guarantee the stability of the 3D FD migration scheme.

Inverting the idea of Kitchenside (1988), who propagated the field using phase shift and the residual using FD, Li (1991) proposed to use conventional FD migration plus a residual field correction by phase shift to improve the migrated image quality. Without any need to modify the conventional 3D FD migration, the Li correction adds a phase-shift filter at certain steps of the downward extrapolation. This technique corrects not only for the splitting error, but also for the positioning error of steeply dipping reflectors.

Biondi (2002) showed that FFD migration is more precise than other methods that use implicit finite differences like pseudoscreen propagators (Jin et al., 1999) and high-angle screen propagators (Xie and Wu, 1998). Given that the computational complexity of all three methods is approximately the same, FFD migration is more attractive than the others. Unfortunately, when conventional FFD migration is applied in the presence of strong velocity contrasts, it can generate numerical instabilities, too.

To overcome the problem of instabilities in models with strong lateral velocity contrasts, Biondi (2002) presented a correction to the FFD method that avoids stability problems. To derive it, he adapted a theory of Godfrey et al. (1979) and Brown (1979), which improves the stability of the 45° equation. The corrected FFD method is unconditionally stable for arbitrary velocity variations, as much in the velocity model as in the reference velocity. Particularly, and differently from conventional FFD migration, it is unconditionally stable even if the reference velocity is smaller than the model velocity. This new property allows for the application of the interpolation technique, conventionally used to improve phase-shift and split-step migration (Gazdag and Sguazzero, 1984) but impossible in FFD migration, because it needs propagation with a larger and a smaller reference velocity. The resulting migration technique is called FFD plus interpolation, or

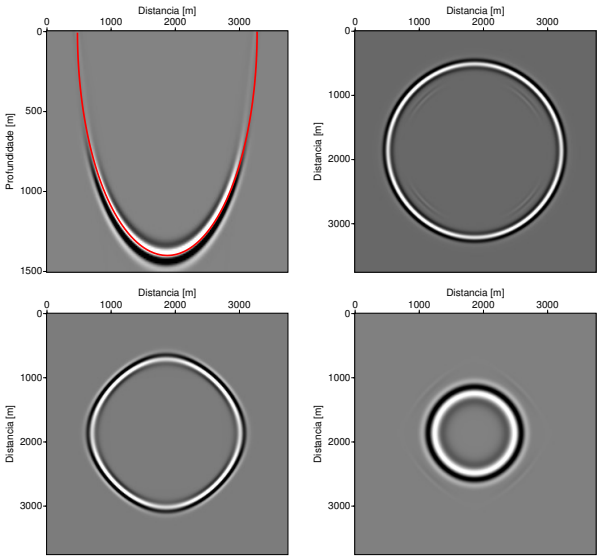

Figure 1: Impulse response of FFD migration using conventional two-way splitting; $p = 0.75$.

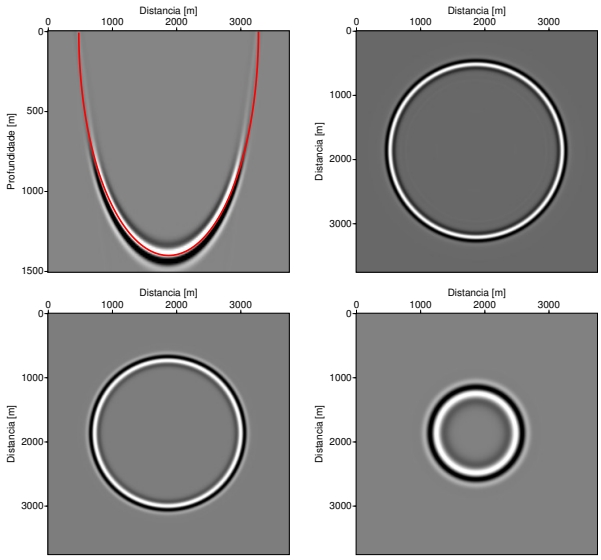

Figure 2: Impulse response of FFD migration using conventional four-way splitting; $p = 0.75$.

shortly FFDPI.

Another, computationally less expensive method to stabilize FFD migration in the presence of strong lateral velocity contrasts was proposed by Amazonas et al. (2007). It substitutes the real Padé approximation (Bamberger et al., 1988) used in the derivation of FFD migration (Ristow and Rühl, 1994) by its complex version (Millinazzo et al., 1997). In this way, the incorrect treatment of near horizontal and slightly evanescent waves of the real Páde approximation is improved, leading to a more stable FFD algorithm, shortly referred to as complex Padé FFD (CPFFD) migration.

In this work, we study possibilities of efficiently implementing these stable FFD migration techniques in 3D. We implemented and compared splitting techniques for FFDPI (Biondi, 2002) and CPFFD (Amazonas et al., 2007) migration. Our numerical tests indicate that a very robust, highly efficient, and satisfactorily accurate method is alternate four-way splitting, i.e., splitting into the coordinate directions at one extrapolation step and into the diagonal directions at the next step.

Numerical experiments

Tests in a homogeneous medium

To study the numerical anisotropy of FFD migration operators after splitting, we calculated impulse-responses for zero-offset migration in a homogeneous medium with velocity 2.5 km/s. The source pulse was a Ricker wavelet with central frequency 25 Hz, with its centre positioned at an arrival time of 0.56 s. The migration grid was $\Delta x = \Delta y = 12.5$ m, and $\Delta z = 10$ m. All our examples used a complex Padé implementation of FFD migration with 3 terms in the series. The value of the reference velocity was chosen as $c_r = 1875$ m/s, i.e., $p = c_r/c(\mathbf{x}) = 0.75$.

Figure 1 shows one vertical and three horizontal cuts through the impulse response of complex Padé FFD migration using conventional two-way splitting. The red line in the top left figure indicates the true theoretical position of the event, given by the half-circle $z = \sqrt{(ct_e)^2 - (x - x_s)^2}$, where t_e is the observation time of the event in the data, here 0.56 s, and x_s is the source position, here the centre of the image, i.e., $x_s = 1850$ m. The non-circular appearance of this line in Figure 1 is caused by the overstretched vertical axis. For a better comparison, we will present all other impulse responses below in the same way.

In the vertical cut (top left), only a slight deformation from circular shape is visible, which is due to the cut being within the coordinate plane, where the errors are the smallest. Note that the amplitude decay at high propagation angles is partly caused by the source implementation, which did not use the amplitude correction of Wapenaar (1990). In the deepest horizontal cut (bottom right), i.e., for propagation directions close to the vertical axis, we observe the well-preserved circular shape of the impulse response. However, the shallow and, principally, medium horizontal cuts reveal a visible deformation, indicating a quality loss for higher propagation angles. Also note the amplitude loss in the directions of the coordinate axes that is visible in the shallow and medium horizontal cuts. The observed behavior will be emphasized in media with strong lateral variations, where much smaller values of p will occur.

Figure 2 shows the impulse response of FFD migration using conventional four-way splitting. The circular shape of the impulse-response has been nicely recovered by the application of the two additional differential operators in the diagonal directions. Also, the amplitude loss in the coordinate directions is no longer visible. Note that this image has about twice the computational cost of the one in Figure 3.

Figure 3 shows the impulse response of CPFFD migration using alternating four-way splitting, i.e., two-way splitting in the coordinate directions at one depth level and in the diagonal directions at the next depth level. It is hard to spot any difference to the result of complete four-way splitting of Figure 2. The circular format of the operator is almost perfect, and even the slight amplitude loss along the coordinate axes is as well recovered as by complete four-way splitting. Note that this image has about the same

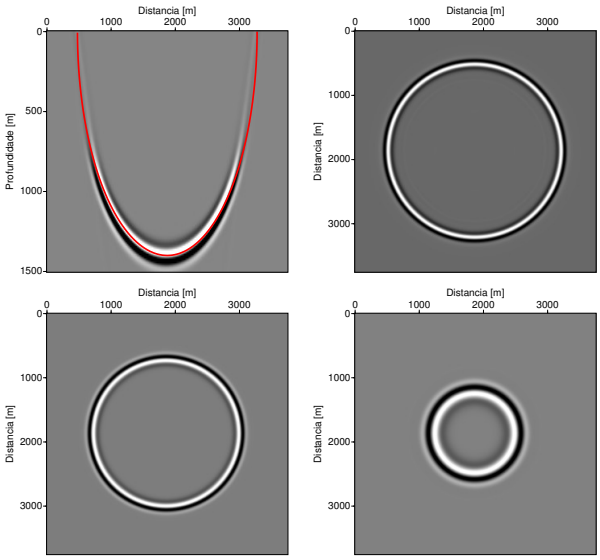

Figure 3: Impulse response of FFD migration using alternating four-way splitting; $p = 0.75$.

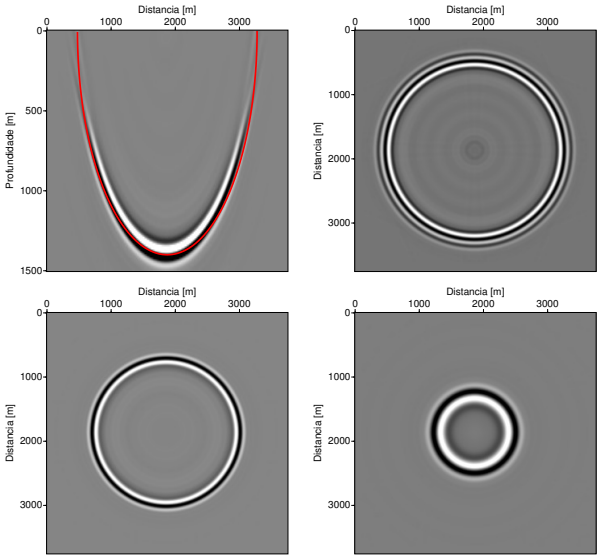

Figure 4: Impulse response of FFDPI migration using conventional two-way splitting, with interpolation between $p = 0.9$ and $p = 1.1$.

computational cost as the one obtained with conventional two-way splitting of Figure 1.

Figure 4 shows the impulse response of FFDPI migration using conventional two-way splitting, with interpolation between wavefields obtained for $p = 0.9$ and $p = 1.1$. We chose these values to reflect the fact that for FFDPI, generally reference velocities closer to the medium velocity are available for interpolation. We observe a good preservation of the circular shape, particularly in the horizontal cuts. In the vertical cut, we note that the wavefront lags slightly behind the true position, starting already at rather low propagation angles of about 35°. The amplitude decay for high propagation angles is reduced as compared to FFD, probably because the reference velocities are closer to the medium velocity than in the previous examples. Finally, the shallowest cut exhibits some numerical dispersion, causing a distorted pulse

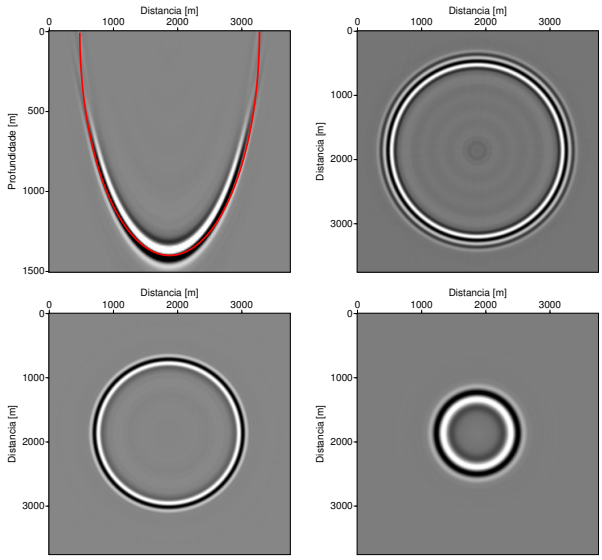

Figure 5: Impulse response of FFDPI migration using alternating four-way splitting, with interpolation between $p = 0.9$ and $p = 1.1$.

shape.

Figure 5 shows the impulse response of FFDPI migration using alternating four-way splitting, with interpolation between wavefields obtained for $p = 0.9$ and $p = 1.1$. Almost no improvement over the conventional two-way splitting result of Figure 4 is visible.

Tests in an inhomogeneous medium

For a more realistic test of the different splitting techniques for FFD migration, we calculated zero-offset impulse responses for the EAGE/SEG salt model. Here, we used a seismic pulse in the centre of the model, described by a Ricker wavelet with central frequency of 15 Hz, dislocated by $t_e = 1.1$ s, and a migration grid with $\Delta x = \Delta y = \Delta z = 20$ m. To avoid spurious events from the spike reflectors, we regularized the model using a 7×7 median filter.

We represent the results by vertical cuts parallel to the y-z plane at $x = 4.14$ km and $x = 6.80$ km, and parallel to the x-z plane at $y = 4.14$ km and $y = 10.22$ km, as well as horizontal cuts at depths $z = 1.7$ m, $z = 2.9$ km, $z = 3.5$ km, and $z = 4.1$ km. Figures 6 and 7 show these cuts through the EAGE/SEG salt model after filtering.

Figures 8 and 9 show the corresponding cuts through the impulse response of FFD migration with two-way splitting, and Figures 10 and 11 those of FFD migration with alternating four-way splitting. The differences between these sets of figures are due to numerical anisotropy, which is not always easy to see at this scale. The most visible difference is the one between the top left images of Figures 9 and 11. The circular shape of three quarters of the wavefront is well preserved in Figure 11, while visibly distorted in Figure 9. Similar distortions are present in the other figure parts. Some events, particularly in the diagonal directions, are slightly more advanced in Figures 10 and 11 than in Figures 8 and 9. Also, some amplitude differences are visible. We refrain from presenting the results of complete four-way splitting, because they look virtually identical to those in Figures 10 and 11.

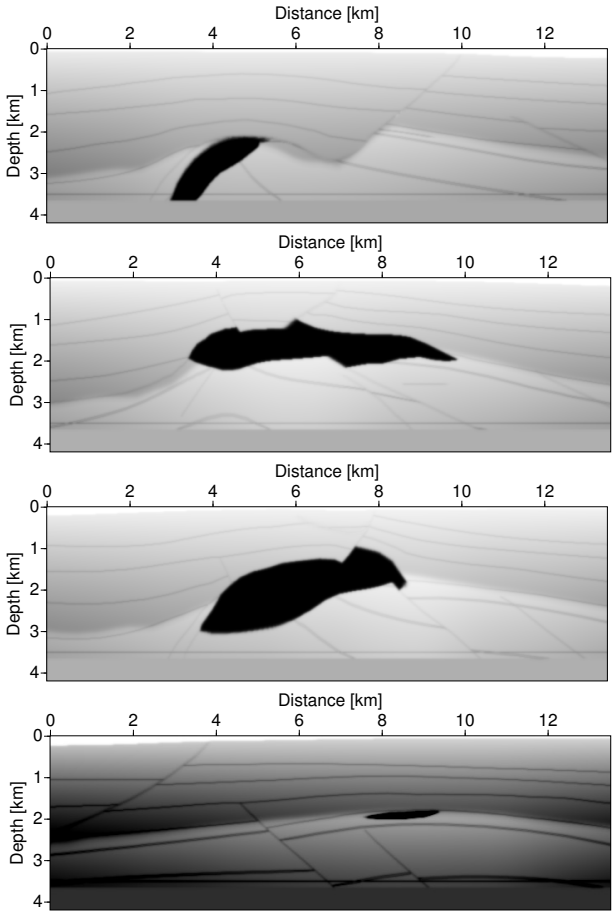

Figure 6: EAGE/SEG salt model. Representation by 4 vertical cuts at $x = 4.14$ km, $x = 6.80$ km (top), $y = 4.14$ km, and $y = 10.22$ km (bottom).

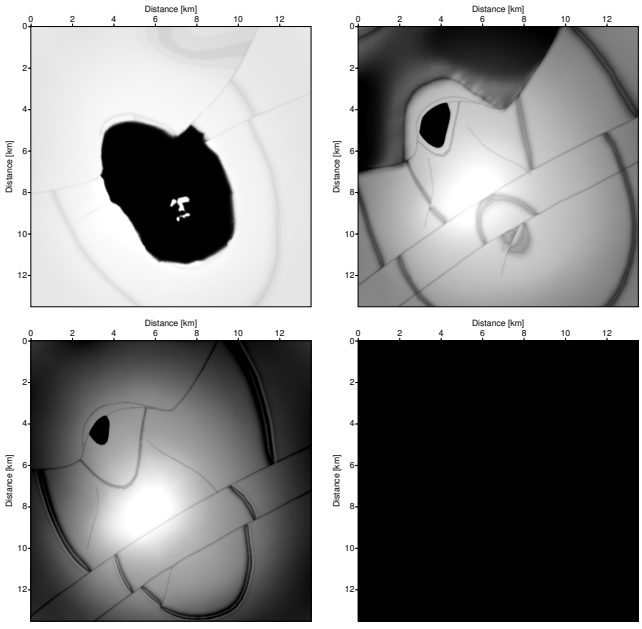

Figure 7: EAGE/SEG salt model. Representation by 4 horizontal cuts at $z = 1.7$ km, $z = 2.9$ km, $z = 3.5$ km, and $z = 4.1$ km (from top left to bottom right).

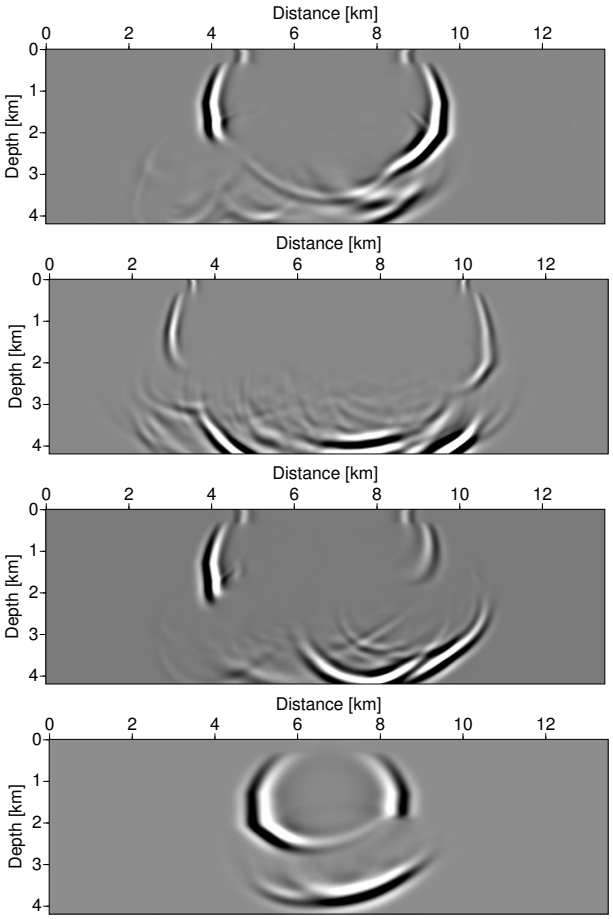

Figure 8: Impulse response of FFD migration with two-way splitting. Cuts as above.

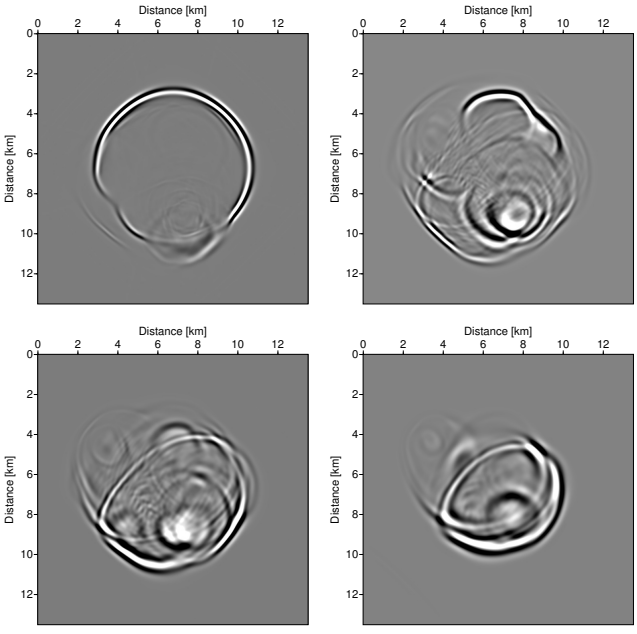

Figure 9: Impulse response of FFD migration with two-way splitting. Cuts as above.

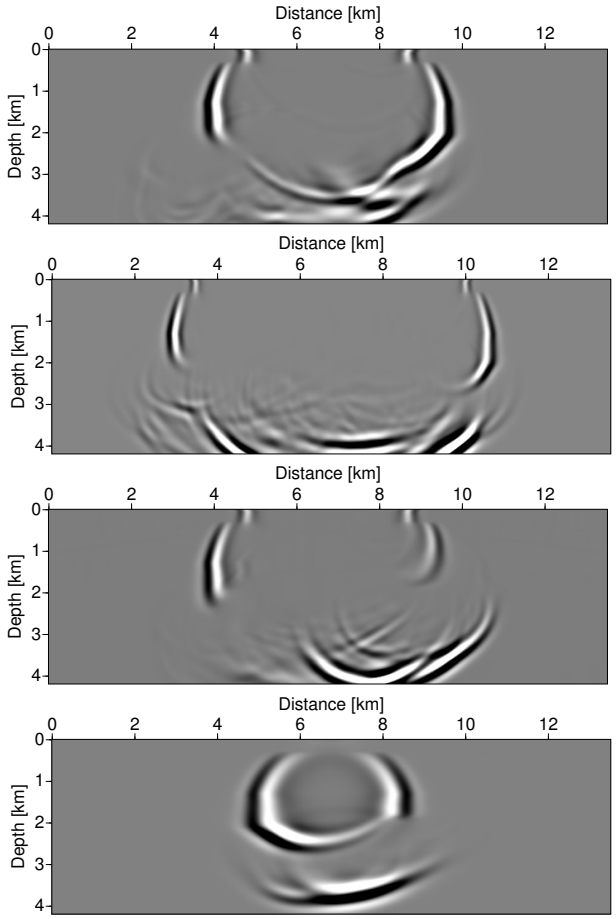

Figure 10: Impulse response of FFD migration with alternating four-way splitting. Cuts as above.

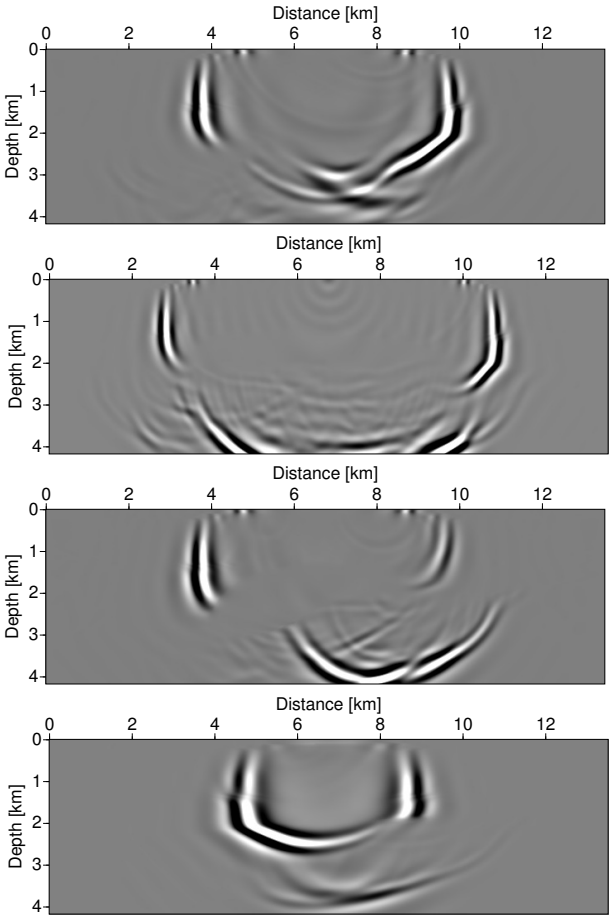

Figure 12: Impulse response of FFDPI migration with two-way splitting using 10 reference velocities. Cuts as above.

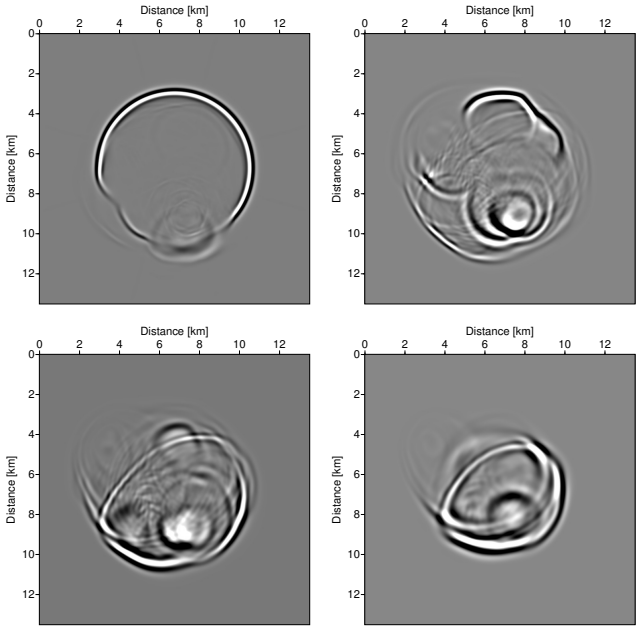

Figure 11: Impulse response of FFD migration with alternating four-way splitting. Cuts as above.

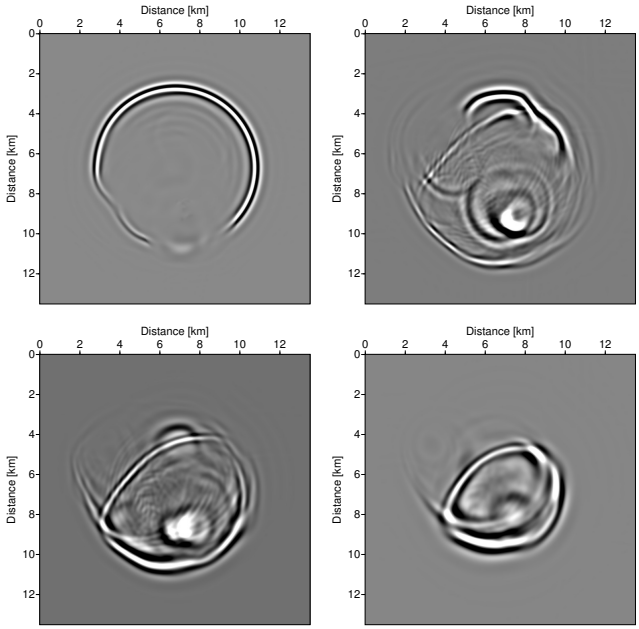

Figure 13: Impulse response of FFDPI migration with two-way splitting using 10 reference velocities. Cuts as above.

For comparison, Figures 12 and 13 show the impulse response of FFDPI migration with two-way splitting. Since the theory of Biondi (2002) is only formulated for a single term of the Padé series, so is our implementation. Because of the strong dependence of FFDPI on reference velocities not too far from the true model velocity, this numerical experiment needed 10 reference velocities. For being a very robust method, the impulse response is not subject to any instabilities, even with the reference velocities being still a bit far from the medium velocities. This remains true even for less reference velocities, though the image quality degrades considerably. Because of the need for a rather large number of reference velocities, FFDPI is a rather expensive method. In our implementation, it used about three times the computational time of alternating four-way FFD.

Even for this experiment with 10 reference velocities, we still see some effects of numerical dispersion in Figures 12 and 13. Also, the results still exhibit quite visible differences to Figures 10 and 11. Since we have at this time no 3D reverse-time migration available, it is hard to tell which results are better positioned. Visual inspection and comparison to results of FD migration (not shown here) make us believe that the FFD results are more reliable than the FFDPI results with 10 reference velocities. More accurate results can be obtained by further increasing the number of reference velocities.

Conclusions

In this paper, we have implemented 3D versions of complex Padé Fourier Finite-Difference (CPFFD) and Fourier Finite-Difference plus interpolation (FFDPI) migrations, which have proven to be more stable in the presence of strong lateral velocity contrasts than other FFD migration implementations. For CPFFD migration, we have compared the effects of different ways of directional splitting and compared its results to those of FFDPI migration. Alternating four-way splitting, i.e., applying the differential operators in the coordinate directions at one depth level and in the diagonal directions at the next depth level, proved to be an improvement over conventional two-way splitting at almost no extra cost. The results were comparable to complete four-way splitting, i.e., all four directions applied at all depth levels. Extensions of the alternating splitting technique can be thought of like eight-way splitting where the remaining directions are covered two by two in the next two depth steps.

From our numerical tests with splitting the CPFFD and FFDPI migration operators, we conclude that FFDPI migration is the most robust of the tested methods. Even implemented only using two-way splitting, it did show only a fair amount of numerical dispersion, but no visible numerical anisotropy. However, in our numerical experiments, the numerical dispersion increased with the difference between the model and reference velocities. Thus, for practical use, FFDPI is a rather expensive method because it needs a large number of reference velocities to function with acceptable precision. For a more economic migration with acceptable image quality, alternating four-way splitting in FFD migration is an interesting alternative.

One minor problem of multi-way splitting should be mentioned. The differential operator in the diagonal directions can cause aliasing effects because of the fact that the grid spacing in this direction is by a factor of $\sqrt{2}$ larger than in the coordinate directions. Off-diagonal directions may complicate things further, because they require resampling.

Acknowledgements

This work was kindly supported by the Brazilian agencies CAPES, FINEP, and CNPq, as well as Petrobras and the sponsors of the *Wave Inversion Technology (WIT) Consortium*.

References

Amazonas, D., J. Costa, J. Schleicher, and R. Pestana, 2007, Wide angle FD and FFD migration using complex Padé approximations: Geophysics, **72**, S215–S220.

Bamberger, A., B. Engquist, L. Halpern, and P. Joly, 1988, Higher order paraxial wave equation approximations in heterogeneous media: J. Appl. Math., **48**, 129–154.

Biondi, B., 2002, Stable wide-angle Fourier finite-difference downward extrapolation of 3-D wavefields: Geophysics, **67**, 872–882.

Brown, D., 1979, Muir's rules for matrices: Another look at stability: Stanford Exploration Project Report, **SEP-20**, 125–142.

Brown, D. L., 1983, Applications of operator separation in reflection seismology: Geophysics, **48**, 288–294.

Claerbout, J. F., 1971, Toward a unified theory of reflector mapping: Geophysics, **36**, 467–481.

Gazdag, J., and P. Sguazzero, 1984, Interval velocity analysis by wave extrapolation: Geophys. Prosp., **32**, 454–479.

Godfrey, R. J., F. Muir, and J. F. Claerbout, 1979, Stable extrapolation: Stanford Exploration Project Report, **SEP-16**, 83–87.

Graves, R. W., and R. W. Clayton, 1990, Modeling acoustic waves with paraxial extrapolators: Geophysics, **55**, 306–319.

Jin, S., R. S. Wu, and C. Peng, 1999, Seismic depth migration with pseudo-screen propagator: Computational Geosciencies, **3**, 321–335.

Kitchenside, P., 1988, Steep dip 3-D migration: Some issues and examples: 58th Annual International Meeting, SEG, Expanded Abstracts, 976–978.

Li, Z., 1991, Compensating finite-difference errors in 3-D migration and modeling: Geophysics, **56**, 1650–1660.

Millinazzo, F. A., C. A. Zala, and G. H. Brooke, 1997, Square-root approximations for parabolic equation algorithms: Journal of the Acoustical Society of America, **101**, 760–766.

Ristow, D., 1980, 3-D downward extrapolation of seismic data in particular by finite difference method: PhD thesis, University of Utrecht.

Ristow, D., and T. Rühl, 1994, Fourier finite-difference migration: Geophysics, **59**, 1882–1893.

———, 1997, 3D implicit finite-difference migration by multiway splitting: Geophysics, **62**, 554–567.

Wapenaar, C. P. A., 1990, Representation of seismic sources in the one-way wave equation (short note): Geophysics, **55**, 786–790.

Xie, X. R., and R. S. Wu, 1998, Improve the wide angle accuracy of screen method under large contrast: 1811–1814.